54456

Wind Tunnel Testing of the NASA-DFRC Flutterometer using a Two DOF Wing Section

Principle Investigator: Thomas W. Strganac, PhD, PE
Graduate Research Assistant: George Platanitis
Department of Aerospace Engineering
Texas A&M University
College Station, Texas 77843-3141

Abstract

Flutter of an aeroelastic structure is potentially destructive aeroelastic instability. This phenomenon has motivated research within the aeroelastic community to develop methods that can accurately predict aeroelastic instabilities. The Flutterometer method used herein, and as developed by NASA DFRC, is based upon the μ method which has been coupled with wavelet filtering processes in estimating aeroelastic models from flight data. The approach leads to a methodology to predict the occurrence of flutter boundaries, and may prove to reliably predict flutter boundaries during flight tests. An analytical model is used as the first estimate of the aeroelastic structural dynamics, and uncertainty operators are introduced into the system to model variations between the theoretical system and the physical system. The modelling uncertainties are then updated from experimental data. Although the model used did not work well with this particular experiment, a sensitivity analysis was additionally performed and improvements suggested.

Introduction

Aeroelasticity is the interaction of structural, inertial, and aerodynamic forces. Together, these forces may cause a structure, such as an aircraft wing, to become unstable and undergo aeroelastic instabilities such as flutter. Among the first to study this characteristic in detail was Theodorsen, and, along with Garrick[1,2], he predicted flutter velocities and frequencies which were compared to experimental results. Several papers have been published on flutter, including methods for its suppression[3,4,5,6]. The exact velocity at which flutter occurs depends on the physical properties of the structure and flow field around it. In the design of aircraft, the study of aeroelastic stability is required in order to determine a safe flight envelope. Many areas have been identified by the flutter community for developing an accurate flutter prediction method, including the time and cost associated with safely expanding the flight envelope in which no aeroelastic instabilities occur[7,8]. Several methods have been used in an attempt to predict flutter. Some of these methods are briefly discussed in Reference 9, 10, and 11 and are presented below. A traditional method analyses system parameters, such as damping to monitor aircraft stability. A prediction-error method was used to estimate damping errors, and extended to use Kalman filtering as well as time-domain and frequency-domain characteristics to estimate damping. But damping may be highly nonlinear as flight conditions vary; therefore, damping trends may be of limited usefulness, as stability may be indicated at a test point, but may not confidently be extrapolated to other flight conditions. Thus the flight envelope must be expanded slowly[12,13,14].

Another method considers the interaction of two modes participating in the flutter mechanism to utilize a stability parameter that is varied quadratically with dynamic pressure[15]. The technique considered several interacting modes and demonstrated a predictive method for higher order instabilities. It was limited though in applicability for general flight flutter testing because assuming only the coupling of a few modes and requiring their observation may be too restrictive[16,17,18].

Stability parameters have also been introduced in flutter margin methods that consider an autoregressive moving average process to describe aeroelastic dynamics[19,20]. While these margins are applicable to complex systems and require only turbulence for excitation, the flutter boundary is determined from the extrapolation of a nonlinear function and may be misleading.

An approach currently being investigated is the use of a nominal model as the initial estimate of the properties of the aeroelastic structure and the incorporation of flight data in the model development process using uncertainty operators in a robust stability framework. The uncertainty operators are incorporated in the model through a linear fractional transformation (LFT), and the robust stability parameter known as the structured singular value[21], μ, is used to calculate flutter boundaries robust to these variations. In this manner, a worst-case flutter boundary is computed which accounts for the flight data directly. Difficulties of estimating a higher order model from data of low signal-to-noise ratio can be avoided, while time-varying dynamics are accounted for by updating the uncertainties between the nominal and true model[10]. The use of the structured singular value has led to this approach being dubbed "μ-method", which is the basis of a flutter-prediction method called the "Flutterometer"[9,11]. The outcome may be immediately realized by on-line computing of robust flutter margins, with the result being the "distance" to the flutter boundary, determined by the largest increase in dynamic pressure (hence, the corresponding increase in velocity), for which the model is robustly stable.

Background on μ - Method Framework

Any aeroelastic model is an approximation of the true system dynamics, but inaccuracies in various model parameters, as well as unmodelled dynamics must be considered in any stability analysis as well as control synthesis[8]. The characteristics of the system model are considered under the influence of perturbations, which contain the parameter uncertainties as well as any unmodelled dynamics or unmeasured forces[7]. The uncertainties are described by an operator, Δ, contained within a set, $\mathbf{\Delta}$, which is norm bounded to reflect the limits of the perturbation sizes. Weighting matrices are often introduced in the μ framework in order to normalize the uncertainty norm bound to unity. Thus, the perturbation set is defined as:

$$\mathbf{\Delta} = \left\{ \Delta : \|\Delta\|_\infty \leq 1 \right\} \tag{1}$$

By the Small Gain Theorem[7,21], the robust stability of a plant model P containing uncertainties is guaranteed for the set $\mathbf{\Delta}$ if $\|P\|_\infty < 1$, though this condition is sufficient but not necessary because it may be overly conservative with respect to structured uncertainty. The equations of motion are rearranged into state-space form, and written as an upper LFT with the uncertainty block structure Δ. The LFT (Figure 1) is formed with uncertainty over velocity,

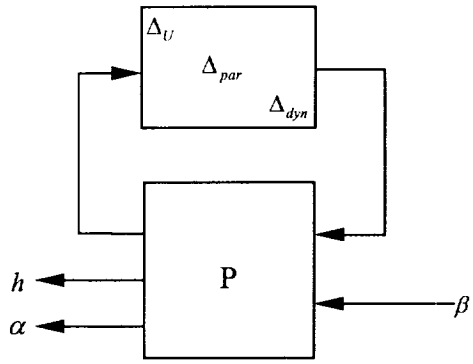

Figure 1. Linear Fractional Transformation block diagram with uncertainty matrix included.

Δ_U, as well as parameter uncertainty, Δ_{par}, and dynamic uncertainty, Δ_{dyn}, (which contains sensor and actuator uncertainties), thus achieving a robust aeroelastic model[3,21,22]. The basis for the μ method is the structured singular value, which is defined as:

$$\mu_{\Delta}(P) = \frac{1}{\min\{\bar{\sigma}(\Delta) : \Delta \in \mathbf{\Delta}, \det(I - P\Delta) = 0\}} \tag{2}$$

and is a measure of the robustness of P with respect to $\mathbf{\Delta}$. The structured singular value, $\mu_{\Delta}(P)$, is a measure of the smallest destabilizing perturbation of P such that $I - P\Delta$ is singular for some $\Delta \in \mathbf{\Delta}$. If no $\Delta \in \mathbf{\Delta}$ exists that makes $I - P\Delta$ singular, then $\mu_{\Delta}(P) := 0$. In effect, the inverse of $\mu_{\Delta}(P)$ is the magnitude of the smallest destabilizing perturbation $\Delta \in \mathbf{\Delta}$. For a unity norm bound set $\mathbf{\Delta}$, the system P is guaranteed to be robustly stable if $\mu_{\Delta}(P) < 1$[7]. The structured singular value is computed numerically as an upper and lower bound using the μ-tools software of MATLAB®.

Model Validation

Robustness measurements are only meaningful if the uncertainty description of a given system model is realistic. Too much uncertainty may cause an overly conservative measure of robustness, while too little uncertainty may generate a robustness measure that does not consider the true errors in the model[7]. It is necessary to validate any given model against a set of experimental data in order to determine a reasonable set of uncertainties. A μ-based method[8,10,11] is used in this paper to validate the robust aeroelastic model of the airfoil pitch-plunge system, which assumes a known model, P, and its associated uncertainty set, $\mathbf{\Delta}$. An uncertainty set is sought such that $F_u(P, \Delta)$ could generate a set of observed data, u (input) and y (output), in frequency space. The plant model is partitioned as follows:

$$P = \begin{bmatrix} P_{11} & P_{12} \\ P_{21} & P_{22} \end{bmatrix} \tag{3}$$

where P_{11} is the transfer function from uncertainty input to uncertainty output, P_{12} the actuator input to uncertainty output, P_{21} the uncertainty input to sensor output, and P_{22} the actuator input to sensor output, which is the nominal plant transfer function. Define the following two matrices:

$$\begin{aligned} \hat{P}_{12} &= P_{12}u \\ \hat{P}_{22} &= P_{22}u - y \end{aligned} \tag{4}$$

The model is not invalidated if the following is true:

$$\mu(P_{11} - \hat{P}_{12}P_{22}^{-1}\hat{P}_{22}) > 1 \tag{5}$$

The above statement may sound counterintuitive, requiring the value of μ to be greater than one to validate the data, while robust stability requires μ to be less than one. Consider the following relationship between u and y:

$$\begin{aligned} 0 &= [P_{22}u - y] + P_{21}\Delta(I - P_{11}\Delta)^{-1}[P_{12}u] \\ &= \hat{P}_{22} + P_{21}\Delta(I - P_{11}\Delta)^{-1}\hat{P}_{12} \end{aligned} \tag{6}$$

where the plant $\hat{P} = \{P_{11}, \hat{P}_{12}, P_{21}, \hat{P}_{22}\}$. The existence of Δ satisfying (6) is equivalent to the plant not being robustly stable, thus, the model is not invalidated by the experimental data if $\mu(\hat{P}) > 1$. In effect, this is an inverted robust stability criterion.

The validation algorithm makes use of three system matrices. The first is P_{true}, which represents the true dynamics of the system and is used to validate a given set of experimental data to determine a realistic set of uncertainties. The second is P_{nom}, which is a theoretical approximation of the system dynamics (derived from the equations of motion), but does not take into account any unmeasured forces or unmodelled dynamics. This matrix is scaled with the uncertainties found using P_{true} in the validation process to give the third matrix, P_{rob}, the system matrix which includes a perturbation in the freestream velocity and is utilized in the μ framework to determine the change in freestream velocity necessary to drive the system to instability.

Equations of Motion for the 2 DOF Model

The implementation of the Flutterometer is demonstrated using a wing section mounted to the Nonlinear Aeroelastic Test Apparatus (NATA)[23] in our wind tunnel (Figures 2 and 3). This system has been used extensively to study both linear and nonlinear aeroelastic motion, as well as develop control strategies[4,5,6,24,25]. The system consists of a wing section mounted on a carriage and is restricted in motion to pitch and plunge degrees of freedom. The bending and torsional modes of the wing are represented by springs and cams, which permit translational and rotational motion. A data acquisition system measures the pitch and plunge dynamics of the system, as well as provide control surface actuation, if applicable to the test. Figure 6 shows the schematic setup of the wing section with the data acquisition system.

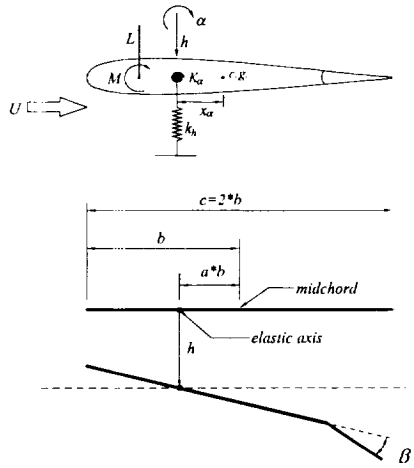

Figure 2. The aeroelastic system permits two degree-of-freedom motion. A control surface is attached tothe trailing edge to provide controlled sinusoidal forces during tests.

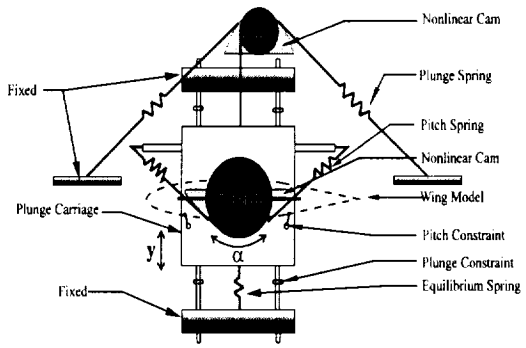

Figure 3. The model support system (NATA) permits prescribed nonlinear motion in two degrees of freedom.

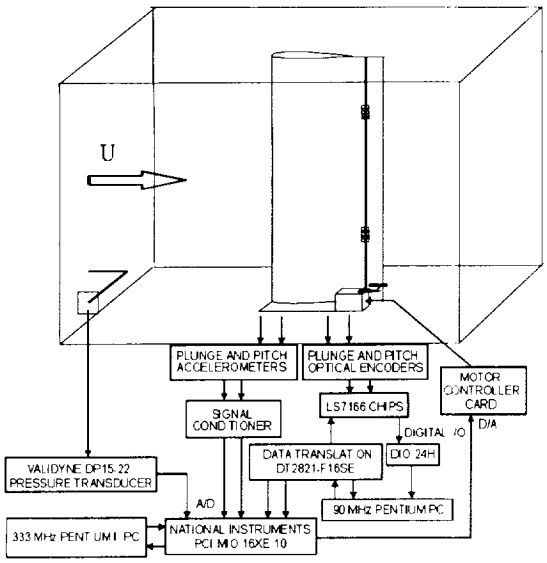

Figure 4. Data acquisition and active control schematic diagram for NATA tests.

Flutter conditions may be reached on this system with minimal concern of structural failure, and parametric investigations of the system characteristics may be conducted, where the effect of changes on stiffness, elastic axis position, mass distributions, as well as various nonlinear features, may be explored. For this investigation, a linearized form of the equations of motion[1] for the wing section mounted to the pitch-plunge system is used:

$$\begin{bmatrix} m_T & m_W x_\alpha b \\ m_W x_\alpha b & I_\alpha \end{bmatrix} \begin{Bmatrix} \ddot{h} \\ \ddot{\alpha} \end{Bmatrix} + \begin{bmatrix} c_h & 0 \\ 0 & c_\alpha \end{bmatrix} \begin{Bmatrix} \dot{h} \\ \dot{\alpha} \end{Bmatrix} + \begin{bmatrix} k_h & 0 \\ 0 & k_\alpha \end{bmatrix} \begin{Bmatrix} h \\ \alpha \end{Bmatrix} = \begin{Bmatrix} -L \\ M \end{Bmatrix} \tag{7}$$

where h and α are the plunge and pitch coordinates respectively, m_T is the total mass of the system, m_W is the mass of the airfoil section, x_α is the nondimensionalized distance from the elastic axis to the center of mass, b is the semi-chord length, c_h and c_α are viscous damping terms, k_h and k_α are the pitch and plunge stiffness, and I_α is the moment of inertia of the airfoil about the elastic axis.

The aerodynamic lift and moment, L and M respectively, are given by:

$$\begin{aligned} L &= \rho U^2 b s C_{l\alpha} \left(\alpha + \frac{\dot{h}}{U} + \left(\frac{1}{2} - a \right) b \frac{\dot{\alpha}}{U} \right) + \rho U^2 b s C_{l\beta} \beta \\ M &= \rho U^2 b^2 s C_{m\alpha} \left(\alpha + \frac{\dot{h}}{U} + \left(\frac{1}{2} - a \right) b \frac{\dot{\alpha}}{U} \right) + \rho U^2 b^2 s C_{m\beta} \beta \end{aligned} \tag{8}$$

where ρ is the air density, U is the freestream velocity of the wind tunnel, s is the airfoil span, a is the nondimensional distance from the midchord to the elastic axis, $C_{l\alpha}$ and $C_{l\beta}$ are lift coefficients, $C_{m\alpha}$ and $C_{m\beta}$ are moment coefficients, and β is the flap deflection. For this experiment, a frequency sweep is used for the control input. The values of all the parameters in the equations are listed below in Table 1.

Table 1: System Parameters

b	0.135 m	m_a	1.664 kg
s	0.6 m	m_f	0.273 kg
r_{cg}	$2(0.3233)b$-b-ab	m_m	0.114 kg
x_α	r_{cg}/b	m_W	$m_a + m_f + m_m$
k_h	2844.4 N/m	m_T	$12 + m_f + m_m$
k_α	3.5895 N.m/rad	I_f	0.00681 kg.m^2
c_h	27.43 N/m	I_m	0.001735 kg.m^2
c_α	0.036 kg.m^2/s	I_α	$0.04325 + I_f + I_m + m_W r_{cg}^2$
ρ	1.225 kg/m^3	$C_{l\beta}$	3.358
$C_{l\alpha}$	6.28	$C_{m\beta}$	-0.635
$C_{m\alpha}$	$(0.5 + a)C_{l\alpha}$		

Here, m_a, m_m, and m_f are the masses of the wing section without the control surface, the servomotor, and the control surface respectively, and I_f and I_m are the mass moments of inertia of the control surface and the servomotor respectively.

The equations of motion are rearranged into state-space form and uncertainties in the parameters are introduced. A detailed derivation of the uncertain model can be found in Reference 26, introducing a perturbation in the freestream velocity, which is used to determine the flutter velocity through μ-analysis, with the main points summarized here. The uncertain plant model corresponds to the following equation:

$$\begin{bmatrix} z_U \\ z_M \\ z_S \\ z_A \\ y \end{bmatrix} = P \begin{bmatrix} w_U \\ w_M \\ w_S \\ w_A \\ \beta \end{bmatrix} \tag{9}$$

where z_U, z_M, z_S, and z_A are input signals to the uncertainty block for freestream velocity, mass, damping and stiffness, and aerodynamic coefficient uncertainty, while w_U, w_M, w_S, and w_A are the uncertainty feedback signals to the plant from the uncertainty block. Equation (9) can be written as an LFT as shown in Figure 5.

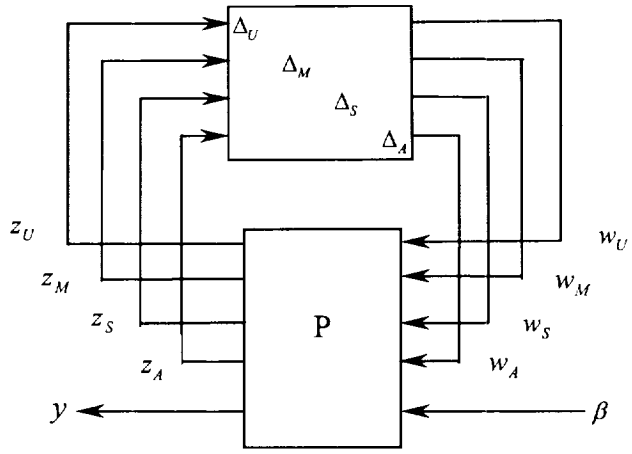

Figure 5. LFT of the uncertainty model for the pitch-plunge system.

where Δ_U, Δ_M, Δ_S, and Δ_A, are the blocks that contain the uncertainties in the parameters. The uncertainty, δ_U, is introduced to the freestream velocity, weighted by W_U:

$$U = U_o + W_U \delta_U \tag{10}$$

and is a convenient mathematical representation that allows operating conditions to be considered by setting δ_U. Similarly, the uncertainties and weights for the mass variables are:

$$\begin{aligned} m_T &= m_{To} + W_{m_T} \delta_{m_T} \\ m_W &= m_{Wo} + W_{m_W} \delta_{m_W} \\ I_\alpha &= I_{\alpha o} + W_{I_\alpha} \delta_{I_\alpha} \end{aligned} \tag{11}$$

and the damping and stiffness uncertainties:

$$\begin{aligned} c_h &= c_{ho} + W_{c_h} \delta_{c_h} \\ c_\alpha &= c_{\alpha o} + W_{c_\alpha} \delta_{c_\alpha} \\ k_h &= k_{ho} + W_{k_h} \delta_{k_h} \\ k_\alpha &= k_{\alpha o} + W_{k_\alpha} \delta_{k_\alpha} \end{aligned} \tag{12}$$

and finally, the aerodynamic parameters:

$$\begin{aligned} C_{l\alpha} &= C_{l\alpha o} + W_{C_{l\alpha}} \delta_{C_{l\alpha}} \\ C_{m\alpha} &= C_{m\alpha o} + W_{C_{m\alpha}} \delta_{C_{m\alpha}} \\ C_{l\beta} &= C_{l\beta o} + W_{C_{l\beta}} \delta_{C_{l\beta}} \\ C_{m\beta} &= C_{m\beta o} + W_{C_{m\beta}} \delta_{C_{m\beta}} \end{aligned} \tag{13}$$

Table 2 shows the initial uncertainty weight scaling factors used for each parameter uncertainty. An input multiplicative uncertainty has also been included in the uncertainty set.

Table 2: Uncertainty Weights for Associated Parameters

W_{m_T}	1
W_{m_w}	1
W_{I_α}	1
W_{c_h}	2
W_{c_α}	0.003
W_{k_h}	140
W_{k_α}	0.17
$W_{C_{l_\alpha}}$	1
$W_{C_{m_\alpha}}$	1
$W_{C_{l_\beta}}$	1
$W_{C_{m_\beta}}$	1
W_{in}	0.2

The Flutterometer

The Flutterometer[9], developed at NASA Dryden Flight Research Center using the MATLAB® μ-Tools software package, was used to determine flutter and instability margins for the wing section. The Flutterometer predicts flutter margins via a program that incorporates the μ-method to validate a system model against experimental data. Wavelet filtering processes have been incorporated with the μ-method for model identification.[27,28] Recently, the Flutterometer has been implemented on-line during flight tests on an F/A-18 research aircraft in which flight data at various test points was gathered and the flutter envelope determined[8]. The use of the F/A-18 explored the advantages of the Flutterometer over traditional methods[8,9]. Using the equations of motion that describe the response of the pitch-plunge system, P_{true} was determined for the freestream velocity of each set of experimental data and an appropriate set of uncertainties was established. The model uncertainties were updated until the experimental data lay between the upper and lower bounds of the structured singular value. The second model, P_{nom}, was also determined as an approximation to the pitch-plunge system at a model velocity, U_{model}. Once an appropriate model was determined, P_{rob} was determined from P_{nom} by scaling P_{nom} with the determined uncertainties and a variation was introduced to the freestream velocity as an additional uncertainty (as shown in Figure 5). Finally, the perturbation in the freestream was evaluated until the system was found to become unstable.

Summary of Results

Two methods were initially used to theoretically evaluate the flutter velocity: i) a classical V-g diagram approach, and ii) a robust stability analysis approach[9] using the structured singular value, μ. For both methods, an analytical model of the pitch-plunge system was used, determined from the equations of motion. For the first approach, an LFT was formed with the nominal model of the system at a given model velocity, U_{model}. An aeroelastic model was evaluated at different values of freestream velocities by varying δ_U (i.e., $U_{model}+\delta_U = U_{new}$), where δ_U is updated by a bisection search. At each new velocity, the eigenvalues of the system are evaluated until the velocity at which the system becomes unstable is reached. In turn, this velocity is used to determine the critical dynamic pressure at which flutter occurs. Figure 6 shows a typical plot of the linear pitch-plunge aeroelastic system, which would undergo flutter motion when reaching a destabilizing velocity. This plot was produced for

k_α = 3.5895 N-m/rad and a = −0.68. Beyond the critical velocity, the two aeroelastic frequencies coalesce thus indicating classical flutter that occurs as seen by the coupling of the two modes[9]. For different physical properties, another type of phenomenon is observed for the same system as shown in Figure 7, where a = −0.4. Rather than under going flutter, the system undergoes aeroelastic divergence[29]. The aeroelastic system fails, due to static instability, when it approaches this velocity. The freestream velocity at which divergence occurs is where one of the modal frequencies reaches zero. For approximately $a < -0.6$, divergence is predicted; for $a \geq -0.6$, classical flutter is predicted. We note that a = −0.5 represents the quarter-chord of the wing, which also represents the aerodynamic center and the center of pressure.

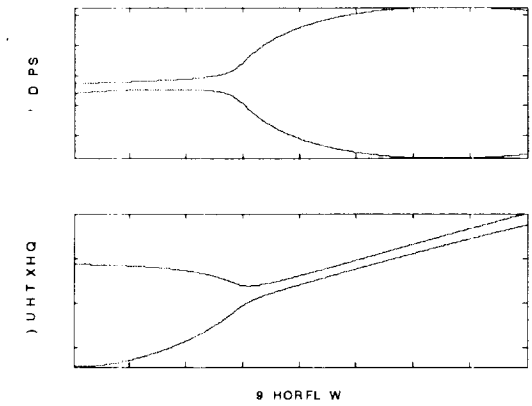

Figure 6. V-g plot for the pitch-plunge system indicating flutter for a = -0.68.

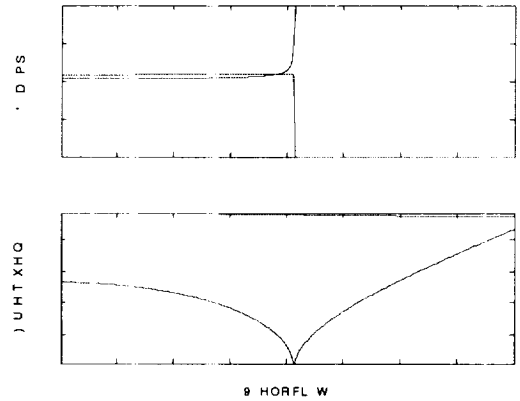

Figure 7. V-g plot for a pitch-plunge system approaching divergence velocity.

The second approach makes use of an LFT of the system with the parametric and dynamic uncertainties, as well as δ_U. For a given model velocity, U_{model}, the uncertain system model is formed. An initial δ_U is chosen and the system is scaled by the uncertainties and by $W_U \delta_U$, as described by equations (10)-(13). The structured singular value, μ, is evaluated for the scaled system and W_U is iteratively updated by W_U / μ to rescale the velocity perturbation (since the velocity is the perturbation parameter of interest, and, applying the definition of μ here, $\mu = 1/(W_U \delta_U)$). The process is repeated until $\mu < 1$. The predicted flutter velocities for each model are summarized in Table 3. For a = −0.68 and U_{model} = 6 m/s, the V-g approach predicted a flutter velocity of 15.1791 m/s while the μ prediction gave 14.304 m/s. Note that for each model velocity, the predicted flutter velocities compare extremely well with the nominal case. No matter what model velocity was used initially, the same flutter velocity could be predicted. For any given initial model velocity, the predicted flutter velocities using

the V-g method agreed within the order of 0.0001 between models as shown in Table 3. While the same type of agreement is desired here, the results from the robust stability analysis differed a little more between models. This difference can be expected since the model is being approximated at each velocity, and uncertainties have been introduced. The flutter velocity predictions obtained from robust stability analysis are always less than the nominal predictions.

Table 3: Predictions of Flutter Velocities for a=-0.68 for the Analytical Model

U_{model} (m/s)	$U_{flutter_{nom}}$ (m/s)	$U_{flutter_{rob}}$ (m/s)
6	15.1791	14.304
7	15.1793	14.386
8	15.1796	14.479

Experiments were then performed for freestream velocities up to ~10 m/s, slowly approaching the flutter velocity, but not actually achieving it. Using simulated data, the Flutterometer predicted flutter velocities of approximately 13 m/s for the linear setup. The system itself has been observed to undergo flutter at a freestream velocity of ~14 m/s on the linear configuration. A command input to the trailing edge control surface was entered (with a steadily increasing frequency) and the response was measured. Initially, the command input was started at 1 Hz and increased 0.5 Hz every 10 cycles for approximately 45 seconds. This frequency selection did not capture the modes between 1.6 and 2.3 Hz (where the natural frequencies of the pitch and plunge modes lie). The first frequency sweep time history is shown in the Figure 8. The frequency sweep was then modified to start at 1.5 Hz and increase by 0.2 Hz every 10 cycles. Figure 9 shows this time history.

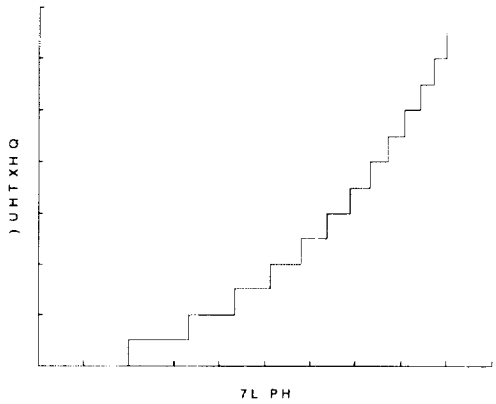

Figure 8. Time history of frequency sweep. A 0.5 Hz change in frequency is provided every 10 cycles. The initial test frequency is 1 Hz.

The experimental data was compared to a simulation from the linear model using the same input history. Some significant differences were noted between the two results, particularly in the pitch mode, as is shown in Figure 10, for a freestream velocity of 9.29 m/s. Interestingly, when the model response was multiplied by 2.5, both data sets compared nicely. It was not understood what caused the differences in amplitude, but the frequencies were in exact agreement.

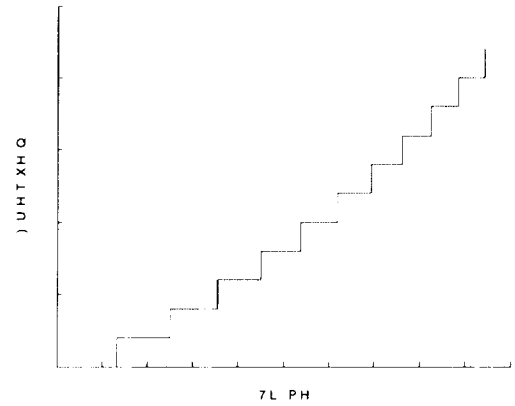

Figure 9. Time history of frequency sweep. A 0.2 Hz change in frequency is provided every 10 cycles. The initial test frequency is 1.5 Hz.

With the experimental data obtained, the Flutterometer showed no convergence (the μ value initially computed was too high and would require a substantial number of iterations for the method to converge, if it was possible for this particular set of data, but was terminated early, with no results obtained). The amount of uncertainty required was too great to place the experimental data within the μ-bounds. See Figures 11 and 12 for the time history of the pitch motion, with the model data included for comparison. Using this disagreeing experimental data in the Flutterometer resulted in a non-convergence of the algorithm to any flutter velocity, and an extremely high computational time.

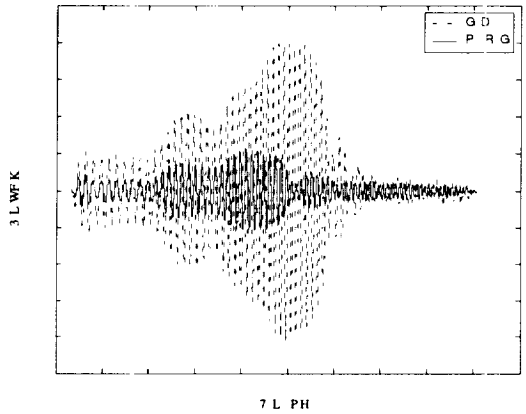

Figure 10: Time response of pitch motion, comparing experimental to simulated response.

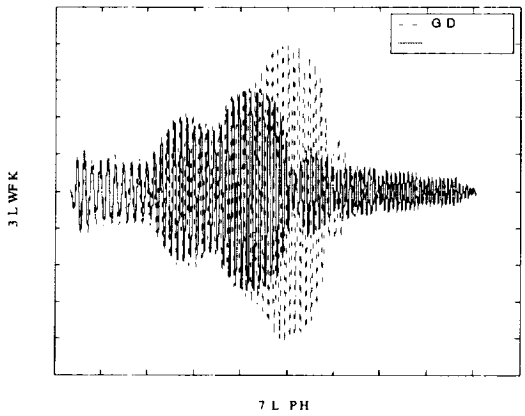

Figure 11: Time response of pitch motion, with model response multiplied by 2.5.

A sensitivity analysis was performed to examine how much error can be introduced into various parameters to determine the quality of the flutter velocity predictions due to model errors. Uncertainties, one at a time, of 30 percent were introduced into the stiffness, mass, viscous damping, and aerodynamic coefficients, and simulated data was produced with this erroneous model. The Flutterometer predicted a flutter velocity of 11.7 m/s. In addition, a 30 percent uncertainty was also introduced into all the aerodynamic coefficients at the same time. Again, the predicted flutter velocity was 11.7 m/s. The Flutterometer showed no sensitivity to the above parameter changes and converged to a flutter velocity. A second sensitivity test was also performed using simulated data by adding random noise at the input and the output to investigate how much error in the data the Flutterometer could tolerate. It was found that if the random noise level added to the simulated data was less than 0.0003, the Flutterometer converged in five iterations to a predicted flutter velocity of 11.7 m/s, else, no convergence was achieved. Note that the above tests were performed for $a = -0.68$.

One explanation for the anomalies seen in Figure 10 is the fact that the model used in the data validation process was valid for small angles of attack. The rather large pitch amplitudes may be affected by aerodynamic stall effects, which contribute to significant nonlinear responses not accounted for in the model. Stall effects are briefly described in Reference 30. This type of behaviour has also been observed in experiments described in Reference 5.

A second explanation is that the commanded deflection for the control surface was not the actual deflection the control surface was undergoing. The wing section model used did not have any method for measuring the true control surface deflection, as the actual deflection would have been more appropriate to use as the input to the system.

Concluding Remarks

A flutter predicting methodology, the Flutterometer, was examined as a technique to predict the occurrence of flutter. Classical predictions were made using a V-g approach and a μ-analysis approach. By using the freestream velocity as an uncertainty parameter, a matched-point solution is achieved for the flutter velocity for the V-g approach, no matter what operating freestream velocity is selected for the model. Using the Flutterometer, an attempt was made to implement experimental data to the Flutterometer. An analytical model was determined for the wing section system at a particular velocity and the uncertainties updated. Unfortunately, since the experimental data did not agree well with the response produced by the model, particularly in the pitch degree of freedom, the result was a non-converging process, with high computational time. A sensitivity analysis showed that the Flutterometer algorithm worked well for small errors. Some of the observed responses, particularly the large pitch amplitudes, could not be adequately explained. In this case, improvements to the current model/experiment hardware associated with our two degree-of-freedom system should be examined.

References

1. Theodorsen, T., "General Theory of Aerodynamic Instability and the Mechanism of Flutter," NACA 496, 1935.

2. Theodorsen, T., and Garrick, I. E., "Mechanism of Flutter: A Theoretical and Experimental Investigation of the Flutter Problem," NACA 685, 1940.

3. Vipperman, J. S., Barker, J. M., Clark, R. L., Balas, J. S. "Comparison of μ- and H_2-Synthesis Controllers on an Experimental Typical Section". *Journal of Guidance, Control, and Dynamics*, Vol. 22, No. 2, 1999, pp. 278-285.

4. O'Neil, T. G. *Experimental and Analytical Investigations of an Aeroelastic Structure With Continuous Nonlinear Stiffness*. Thesis, Department of Aerospace Engineering, Texas A&M University, May 1996.

5. Block, J. J. *Active Control of an Aeroelastic Structure*. Thesis, Department of Aerospace Engineering, Texas A&M University, May 1996.

6. Ko, J., Kurdila, A. J., and Strganac, T. W. "Nonlinear Control of a Prototypical Wing Section with Torsional Nonlinearity". *Journal of Guidance, Control, and Dynamics*, Vol. 20, No. 6, 1997, 1181-1189.

7. Lind, R., Brenner, M. "Incorporating Flight Data into a Robust Aeroelastic Model". *Journal of Aircraft*, Vol. 35, No. 3, 1998, pp. 470-477.

8. Lind, R., Brenner, M. "Robust Flutter Margins of an F/A-18 Aircraft from Aeroelastic Flight Data". *Journal of Guidance, Control, and Dynamics*, Vol. 20, No. 3, 1997, pp. 597-604.

9. Lind, R., Brenner, M. *Robust Aeroservoelastic Stability Analysis – Advances in Industrial Control*. c. 1999 Springer-Verlag London Limited.

10. Lind, R., Brenner, M. J. "A Worst-Case Approach for On-Line Flutter Prediction". *International Forum on Aeroelasticity and Structural Dynamics*, Rome, Italy, June 1997, Volume 2, pp.79-86.

11. Lind, R., and Brenner, J., "Flutterometer: An On-line Tool to Predict Robust Flutter Margins". *Journal of Aircraft*, Vol. 37, No. 6, 2000, pp. 1105-1112.

12. Kehoe, M. W., "A Historical Overview of Flight Flutter Testing," Proceedings of the 80th AGARD Structures and Materials Panel, AGARD-CP-566, Rotterdam, The Netherlands, May 8-10, 1995, pp. 1-15.

13. Roy, R. and Walker, R., *Real-Time Flutter Identification*, NASA-CR-3933, Oct. 1985.

14. Ruhlin, C. L., Watson, J. J., Ricketts, R. H., and Doggett, R. V., "Evaluation of Four Subcritical Response Methods for On-Line Prediction of Flutter Onset in Wind Tunnel Tests," *Journal of Aircraft*, Vol. 20, No. 10, October 1983, pp. 835-840.

15. Zimmerman, N. H. and Weissenburger, J. T., "Prediction of Flutter Onset Speed Based on Flight Testing at Subcritical Speeds," *Journal of Aircraft*, Vol. 1, No. 4, July-August 1964, pp. 190-202.

16. Price, S. J. and Lee, B. H. K., "Development and Analysis of Flight Flutter Prediction Methods," *AIAA Dynamics Specialists Conference*, Dallas, TX, April 1992, AIAA-92-2101, pp. 188-200.

17. Price, S. J. and Lee, B. H. K., "Evaluation and Extension of the Flutter-Margin Method for Flight Flutter Prediction," *Journal of Aircraft*, Vol. 30, No. 3, May-June 1993, pp. 395-402.

18. Kadrnka, K. E., "Multimode Instability Prediction Method," *AIAA Structural Dynamics and Materials Conference*, Orlando, FL, April 1985, AIAA-85-0737, Volume 2, pp. 435-442.

19. Matsuzaki, Y. and Ando, Y., "Estimation of Flutter Boundary from Random Responses Due to Turbulence at Subcritical Speeds," *Journal of Aircraft*, Vol. 18, No.10, October 1981, pp. 862-868.

20. Matsuzaki, Y. and Ando, Y., "Divergence Boundary Prediction from Random Responses: NAL's Method," *Journal of Aircraft*, Vol. 21, No. 6, June 1984, pp. 435-436.

21. Zhou, K., Doyle, J., Glover, K. *Robust and Optimal Control.* C. 1996 by Prentice-Hall, Inc.

22. Balas, G. J., Doyle, J. C., Glover, K., Packard, A., Smith, R. *μ-Analysis and Synthesis Toolbox.* C. 1984-1998 by MUSYN Inc. and The MathWorks, Inc.

23. Thompson, David. *Appendix - Nonlinear Aeroelastic Test Apparatus (NATA).* Internal publication, Department of Aerospace Engineering, Texas A&M University, June 25, 1999.

24. Ko, J., Strganac, T. W., Kurdila, A. J. "Adaptive Feedback Linearization for the Control of a Typical Wing Section With Structural Nonlinearity". c. 1999 Kluwer Academic Publishers. *Nonlinear Dynamics 18*: 289-301.

25. Strganac, T. W., Ko, J., and Thompson, David E., "Identification and Control of Limit Cycle Oscillations in Aeroelastic Systems," *Journal of Guidance, Control, and Dynamics*, Vol. 23, No. 6, November-December 2000.

26. Lind, Rick, *Robust Flutter Analysis of a Pitch-Plunge System.* Internal publication, NASA Dryden Flight Research Center, January 25, 2001.

27. Brenner, M. J., Lind, R. "On-line Robust Modal Stability Prediction Using Wavelet Filtering". *21st Congress of the International Council of Aeronautical Sciences*, Melbourne, Australia, September 13-18, 1998 ICAS-98-4.9.1

28. Brenner, M., Lind, R. "Wavelet Filtering to Reduce Conservatism in Aeroservoelastic Robust Stability Margins". *AIAA Structures, Structural Dynamics, and Materials Conference*, Long Beach CA, April 1998, AIAA-98-1896.

29. Fung, Y. C., *An Introduction to the Theory of Aeroelasticity*, Dover Publications, New York, 1993, pp. 81-85.

30. Kurdila, A. J., Prazenica, R. J., Rediniotis, O., and Strganac, T., "Multiresolution Methods for Reduced-Order Models for Dynamical Systems," *Journal of Guidance, Control, and Dynamics*, Vol. 24, No. 2, 2001, pp. 193-199.